

N-Aryl Chromophore Ligands for Bright Europium Luminescence

Nail M. Shavaleev,[†] Svetlana V. Eliseeva,[†] Rosario Scopelliti,[†] and Jean-Claude G. Bünzli^{*,†,‡}

[†]École Polytechnique Fédérale de Lausanne, Laboratory of Lanthanide Supramolecular Chemistry, BCH 1405, CH-1015 Lausanne, Switzerland, and [‡]World Class University (WCU) Professor, Department of Advanced Materials Chemistry, Center for Next Generation Photovoltaic Systems, Korea University, 208 Seochang, Jochiwon, ChungNam 339-700, South Korea

Received January 22, 2010

Sterically hindered *N*-aryl-benzimidazole pyridine-2-carboxylic acids (aryl = phenyl, 4-biphenyl, 2-naphthyl) readily form homoleptic, neutral, nine-coordinate europium complexes which display efficient sensitized luminescence in solid state and in dichloromethane solution with quantum yields reaching 59% and have monoexponential and nearly temperature-independent lifetimes as long as 2.7 ms. The ligand-centered absorption band with a maximum at 321–342 nm and intensity $(50–56) \times 10^3 \text{ M}^{-1} \text{ cm}^{-1}$ ensures efficient harvesting of excitation light by the complexes. Variation of *N*-aryl chromophore enhances the ligand absorption at 250–350 nm without changing its triplet state energy which amounts to $(19.2–21.3) \times 10^3 \text{ cm}^{-1}$. Photophysical properties of europium complexes benefit from adequate protection of the metal by the ligands against non-radiative deactivation and efficient ligand-to-metal energy transfer exceeding 70%. A correlation is observed between the sensitized luminescence quantum yields of europium and the ligand triplet state energy; in certain cases it points to the presence of a second-sphere quenching of Eu^{III} by co-crystallized water in the solid state.

Introduction

Trivalent europium ion displays orange or red luminescence prompting the use of its inorganic and organic compounds in display, lighting (including OLED), and sensor applications.^{1–4} Although europium luminescence is long-lived, in the μs -ms time scale, it is not quenched by oxygen, as the excited state is located on the shielded f-orbitals of the ion which advantageously distinguishes it from brightly phosphorescent transition metal complexes with charge-transfer (MLCT, LLCT) or ligand-centered emissive states.^{5–9}

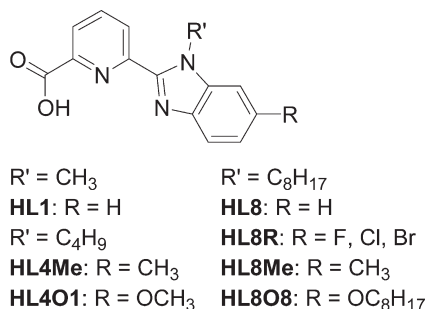
Weak absorption transitions of Eu^{III} necessitates the use of chromophore ligands to achieve efficient harvesting of excitation light.¹⁰ The ligand must have suitable excited states

to transfer energy to the Eu^{III} ion; its first triplet state is generally responsible for most of the energy transfer,^{11,12} but singlet-state excitation may also play a non-negligible role.¹³ It is also desirable that the ligand saturates the coordination sphere of europium, therefore protecting it from water molecules which strongly coordinate to the “hard” Eu^{III} cation and quench its excited state.¹⁴ A number of ligands have been developed to achieve bright luminescence of europium,^{15–27} the most studied ones being bidentate β -diketonates.²⁸

*To whom correspondence should be addressed. E-mail: jean-claude.bunzli@epfl.ch.

- (1) Eliseeva, S. V.; Bünzli, J.-C. G. *Chem. Soc. Rev.* **2010**, *39*, 189.
- (2) Armelao, L.; Quici, S.; Barigelletti, F.; Accorsi, G.; Bottaro, G.; Cavazzini, M.; Tondello, E. *Coord. Chem. Rev.* **2010**, *254*, 487.
- (3) Binnemans, K. *Chem. Rev.* **2009**, *109*, 4283.
- (4) Katkova, M. A.; Vitukhnovsky, A.; Bochkarev, M. N. *Russ. Chem. Rev.* **2005**, *74*, 1089.
- (5) Evans, R. C.; Douglas, P.; Winscom, C. J. *Coord. Chem. Rev.* **2006**, *250*, 2093.
- (6) Lowry, M. S.; Bernhard, S. *Chem.—Eur. J.* **2006**, *12*, 7970.
- (7) Djurovich, P. I.; Murphy, D.; Thompson, M. E.; Hernandez, B.; Gao, R.; Hunt, P. L.; Selke, M. *Dalton Trans.* **2007**, 3763.
- (8) Williams, J. A. G.; Develay, S.; Rochester, D. L.; Murphy, L. *Coord. Chem. Rev.* **2008**, *252*, 2596.
- (9) Baranoff, E.; Yum, J. H.; Graetzel, M.; Nazeeruddin, M. J. *Organomet. Chem.* **2009**, *694*, 2661.
- (10) Weissman, S. I. *J. Chem. Phys.* **1942**, *10*, 214.

- (11) Sato, S.; Wada, M. *Bull. Chem. Soc. Jpn.* **1970**, *43*, 1955.
- (12) Latva, M.; Takalo, H.; Mukkala, V. M.; Matachescu, C.; Rodriguez-Ubis, J.-C.; Kankare, J. *J. Lumin.* **1997**, *75*, 149.
- (13) Ha-Thi, M. H.; Delaire, J. A.; Michelet, V.; Leray, I. *J. Phys. Chem. A* **2010**, *114*, 3264.
- (14) Beeby, A.; Clarkson, I. M.; Dickins, R. S.; Faulkner, S.; Parker, D.; Royle, L.; de Sousa, A. S.; Williams, J. A. G.; Woods, M. *J. Chem. Soc., Perkin Trans. 2* **1999**, 493.
- (15) Andreiadis, E. S.; Demadrille, R.; Imbert, D.; Pecaut, J.; Mazzanti, M. *Chem.—Eur. J.* **2009**, *15*, 9458.
- (16) D'Aléo, A.; Picot, A.; Baldeck, P. L.; Andraud, C.; Maury, O. *Inorg. Chem.* **2008**, *47*, 10269.
- (17) D'Aléo, A.; Moore, E. G.; Szigethy, G.; Xu, J.; Raymond, K. N. *Inorg. Chem.* **2009**, *48*, 9316.
- (18) de Bettencourt-Dias, A.; Viswanathan, S.; Rollett, A. *J. Am. Chem. Soc.* **2007**, *129*, 15436.
- (19) Kadjane, P.; Starck, M.; Camerel, F.; Hill, D.; Hildebrandt, N.; Ziessel, R.; Charbonnière, L. *J. Inorg. Chem.* **2009**, *48*, 4601.
- (20) Kottas, G. S.; Mehlstäubl, M.; Fröhlich, R.; De Cola, L. *Eur. J. Inorg. Chem.* **2007**, 3465.
- (21) Miyata, K.; Hasegawa, Y.; Kuramochi, Y.; Nakagawa, T.; Yokoo, T.; Kawai, T. *Eur. J. Inorg. Chem.* **2009**, 4777.

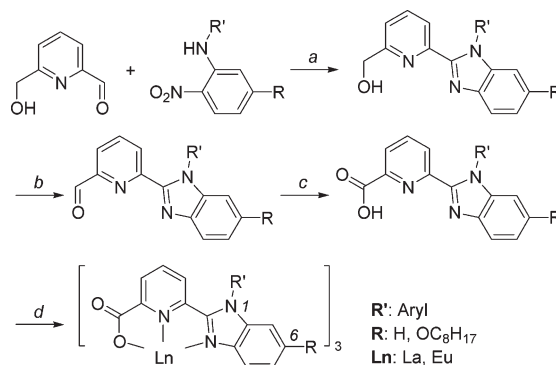
Chart 1. Previously Reported *N*-Alkyl-Benzimidazole Pyridine-2-Carboxylic Acids^{30,31}

We have recently reported that tridentate *N*-alkyl-benzimidazole-pyridine carboxylates²⁹ (Chart 1) form neutral homoleptic complexes with europium and sensitize its emission with quantum yields reaching 71%.^{30,31} To modulate the light-harvesting properties of the ligands we set out to modify them with a strongly absorbing aryl chromophore at the N(1) atom of benzimidazole instead of a “transparent” alkyl group (Scheme 1 and Chart 2; compare with Chart 1). It should be noted that *N*-aryl benzimidazole-pyridines have been rarely used in coordination chemistry^{32,33} likely because of the anticipated steric hindrance to metal binding. Herein we demonstrate that these ligands are easily accessible, readily coordinate to europium, and efficiently sensitize its luminescence.

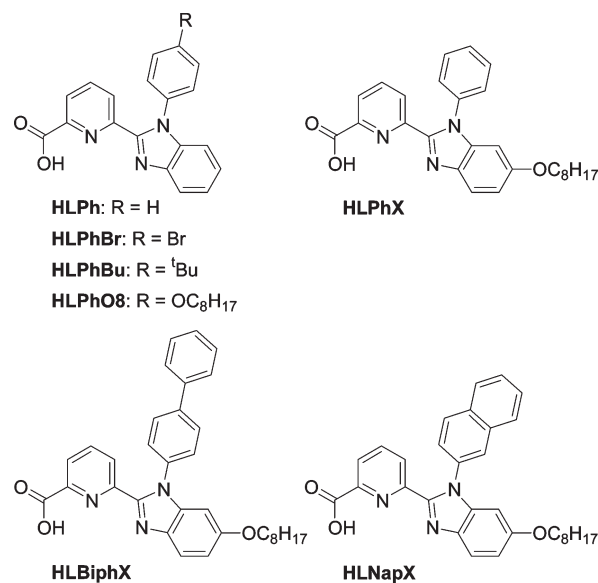
Results and Discussion

Synthesis. Six new ligands have been prepared (Chart 2); the formation of benzimidazole ring³⁴ was followed by stepwise oxidation of pyridine-2-methanol first to carboxaldehyde with SeO_2 , and then to carboxylic acid with H_2O_2 /formic acid³⁵ (Scheme 1). The cyclization of *N*-aryl benzimidazoles was less efficient compared to *N*-alkyl ones³¹ as a result of steric hindrance, while both oxidation steps were high-yielding.

N-Aryl-2-nitroanilines (key precursors) were obtained by reaction of 2-fluoronitrobenzenes with arylamines (used as a reagent and a base) in dimethyl sulfoxide

Scheme 1. Synthesis of *N*-Aryl-Benzimidazole Pyridine-2-Carboxylic Acids and Their Lanthanide Complexes^{a,b}

^a Benzimidazole ring numbering is indicated in the structure of the complex. ^b Reaction conditions: (a) $\text{Na}_2\text{S}_2\text{O}_4$, [2-methoxyethanol and/or DMF]/ H_2O , under N_2 , 110 °C; (b) SeO_2 , dioxane, under N_2 , 110 °C; (c) H_2O_2 , formic acid, under air, 0 °C; (d) $\text{LnCl}_3 \cdot n\text{H}_2\text{O}$, NaOH, ethanol/ H_2O , under air, heating.

Chart 2. *N*-Aryl-Benzimidazole Pyridine-2-Carboxylic Acids^a

^a Ligand HLPh has been reported;³⁰ other ligands are new.

(DMSO) at 100 °C for 24–48 h (Scheme 2). The reaction did not require external base or a catalyst; however, in the case of electron-deficient 4-bromoaniline, it was sluggish and had to be carried out for 72 h. A facile multigram-scale synthesis of another precursor, 2-pyridinecarboxaldehyde-6-methanol, has been previously described.³⁶

The complexes $[\text{Ln}(\text{Ligand})_3] \cdot n\text{H}_2\text{O}$, denoted as **LnLi-gand**, have been obtained as air- and moisture-stable white solids from hot ethanol/water solutions starting with a stoichiometric 3:3:1 molar ratio of ligand, NaOH (base), and $\text{LnCl}_3 \cdot n\text{H}_2\text{O}$ (Scheme 1 and Chart 2). They are soluble in DMSO, and the ones containing *tert*-butyl or *n*-octyloxy groups are also soluble in CH_2Cl_2 . All new compounds have been identified by C, H, N elemental analysis; X-ray crystallography; ¹H and ¹³C NMR spectroscopy; and ESI⁺ MS.

(36) Shavaleev, N. M.; Scopelliti, R.; Gumy, F.; Bünzli, J.-C. G. *Inorg. Chem.* **2009**, *48*, 6178.

(22) Pavithran, R.; Saleesh Kumar, N. S.; Biju, S.; Reddy, M. L. P.; Junior, S. A.; Freire, R. O. *Inorg. Chem.* **2006**, *45*, 2184.

(23) Teotonio, E. E. S.; Brito, H. F.; Viertler, H.; Faustino, W. M.; Malta, O. L.; de Sá, G. F.; Felinto, M. C.; Santos, R. H. A.; Cremona, M. *Polyhedron* **2006**, *25*, 3488.

(24) Wilkinson, A. J.; Maffeo, D.; Beeby, A.; Foster, C. E.; Williams, J. A. G. *Inorg. Chem.* **2007**, *46*, 9438.

(25) Zebret, S.; Dupont, N.; Bernardinelli, G.; Hamacek, J. *Chem.—Eur. J.* **2009**, *15*, 3355.

(26) Zhang, F. L.; Hou, Y. H.; Du, C. X.; Wu, Y. J. *Dalton Trans.* **2009**, 7359.

(27) Sivakumar, S.; Reddy, M. L. P.; Cowley, A. H.; Vasudevan, K. V. *Dalton Trans.* **2010**, *39*, 776.

(28) de Sá, G. F.; Malta, O. L.; Donega, C. D.; Simas, A. M.; Longo, R. L.; Santa-Cruz, P. A.; da Silva, E. F. *Coord. Chem. Rev.* **2000**, *196*, 165.

(29) Piguet, C.; Bocquet, B.; Hopfgartner, G. *Helv. Chim. Acta* **1994**, *77*, 931.

(30) Shavaleev, N. M.; Scopelliti, R.; Gumy, F.; Bünzli, J.-C. G. *Inorg. Chem.* **2009**, *48*, 5611.

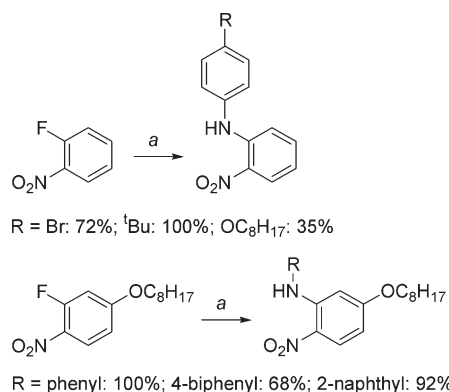
(31) Shavaleev, N. M.; Eliseeva, S. V.; Scopelliti, R.; Bünzli, J.-C. G. *Chem.—Eur. J.* **2009**, *15*, 10790.

(32) Jia, W. L.; McCormick, T.; Tao, Y.; Lu, J. P.; Wang, S. *Inorg. Chem.* **2005**, *44*, 5706.

(33) He, L.; Qiao, J.; Duan, L.; Dong, G.; Zhang, D.; Wang, L.; Qiu, Y. *Adv. Funct. Mater.* **2009**, *19*, 2950.

(34) Yang, D. L.; Fokas, D.; Li, J. Z.; Yu, L. B.; Baldino, C. M. *Synthesis* **2005**, 47.

(35) Dodd, R.; Le Hyaric, M. *Synthesis* **1993**, 295.

Scheme 2. Synthesis of Precursors^a

^a Reaction conditions: (a) arylamine (excess, used as a reagent and as a base), DMSO, under N₂, 24–72 h, 100 °C.

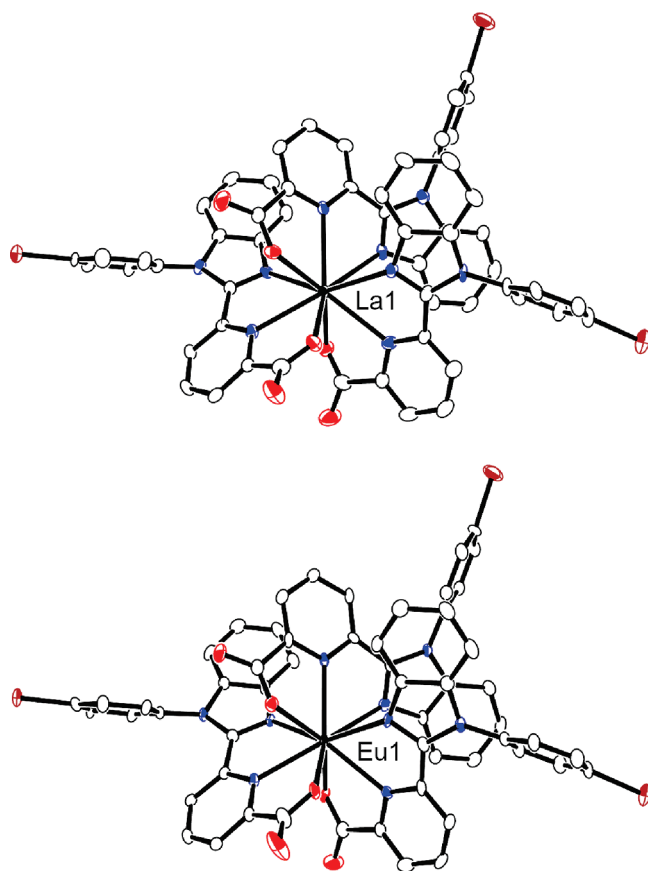


Figure 1. Molecular structures of the complexes [Ln(LPhBr)₃] (Ln = La, Eu) viewed down the triangular face of the tricapped trigonal prism (50% probability ellipsoids, H atoms, and co-crystallized solvent molecules omitted). Heteroatoms: O, red; N, blue; Br, brown; Ln, black.

The following *N*-aryl groups have been chosen as chromophores: phenyl (Ph), 4-biphenyl (Biph), or 2-naphthyl (Nap). The presence of bromine in ligand HPhBr and its precursors opens the way for coupling reactions as means of further modification. The *n*-octyloxy group at *N*-phenyl (HPhO8) or at benzimidazole (HLRX), apart from providing solubility, demonstrates a facile attachment of a functional group to the ligand via ether linkage starting from a suitable phenol precursor. It should be noted that the parent ligand HPh and its complexes have been reported previously.³⁰

Table 1. Selected Structural Parameters of the Complexes^a

complex	bond lengths (Å) ^b			angle (deg) ^c		Ln–Ln (Å) ^d
	Ln–O	Ln–N(py)	Ln–N(b)	py–b	ph–b	
[La(LPhBr) ₃]	2.422(5)	2.638(6)	2.761(5)	28.75	61.57	9.663
	2.453(5)	2.655(6)	2.709(5)	23.53	57.56	
	2.465(5)	2.676(6)	2.778(6)	25.90	60.85	
	2.447(44)	2.656(38)	2.749(72)	26(5)	60(4)	
	<i>0.043</i>	<i>0.038</i>	<i>0.069</i>	5	4	
[Eu(LPhBr) ₃]	2.339(4)	2.535(5)	2.681(5)	27.00	61.17	9.665
	2.358(4)	2.553(5)	2.630(5)	24.86	55.71	
	2.389(4)	2.571(5)	2.688(5)	24.31	60.49	
	2.362(50)	2.553(36)	2.666(63)	25(3)	59(6)	
	<i>0.050</i>	<i>0.036</i>	<i>0.058</i>	3	5	

^a Each row corresponds to one and the same ligand in the complex. Numbers in bold are for averaged data (with standard deviations 2σ in parentheses); numbers in bold and in italic are differences between the minimum and the maximum values. ^b N(py) and N(b) are nitrogen atoms of pyridine and benzimidazole rings, respectively. ^c Dihedral angles between the planes of pyridine and benzimidazole, or benzimidazole and phenyl (ph) rings. The planes were defined by C and N atoms of core rings. ^d Shortest Ln–Ln distance in the structure.

Structural Characterization. Single crystals suitable for X-ray analysis could be obtained for [Ln(LPhBr)₃] (Ln = La, Eu); their molecular structures are shown in Figure 1, and selected parameters are collected in Table 1. The complexes share similar structural properties. The lanthanide ion is 9-coordinate by three ligands, and its coordination polyhedron can be described as a distorted tricapped trigonal prism (TCTP, Figure 2), with N(py = pyridine) atoms in capping positions and forming a plane with Ln. Two triangular faces of the prism are defined by O–N(b)–N(b) and O–O–N(b) atoms (b = benzimidazole). Each of the three ligands spans both triangular faces of the TCTP via a capping position. The ligands are arranged in up-up-down fashion around the metal resulting in low symmetry (C₁) of the complex.

The coordinated ligands are not planar, with dihedral angles between pyridine and benzimidazole in the range 24–29°, while the angles between phenyl and benzimidazole are 56–62°. The three ligands in the complex are not equally strongly bonded to the metal as reflected in the different respective sets of bond lengths. The metal is preferentially bound to the pyridine-2-carboxylate moiety, while bonding to the benzimidazole is weaker, which is reflected in longer bond lengths and in their wider variation. The bond lengths decrease as La > Eu because of lanthanide contraction.

Each ligand of the complex is hydrogen bonded to co-crystallized ethanol or water molecules via carbonyl oxygen of a carboxylate group with O···O(water or ethanol) distances in the range 2.704–2.952 Å. Both structures contain eight Ln···O(7 water + 1 ethanol) distances in the range 6.0–8.0 Å which may result in second-sphere interaction between metal ion and O–H oscillators. Intermetallic communication in the structures is likely to be negligible as the Ln–Ln distances are > 9.6 Å, a favorable condition for efficient luminescence.

The structures of the *N*-aryl complexes are very similar to the previously reported *N*-alkyl complexes.³¹ The only notable difference is that the angles between pyridine and benzimidazole show very small variation in *N*-aryl complexes with average and (2σ) values of 26(4) for LnLPhBr, while in *N*-alkyl complexes they vary as 2–40°.³¹

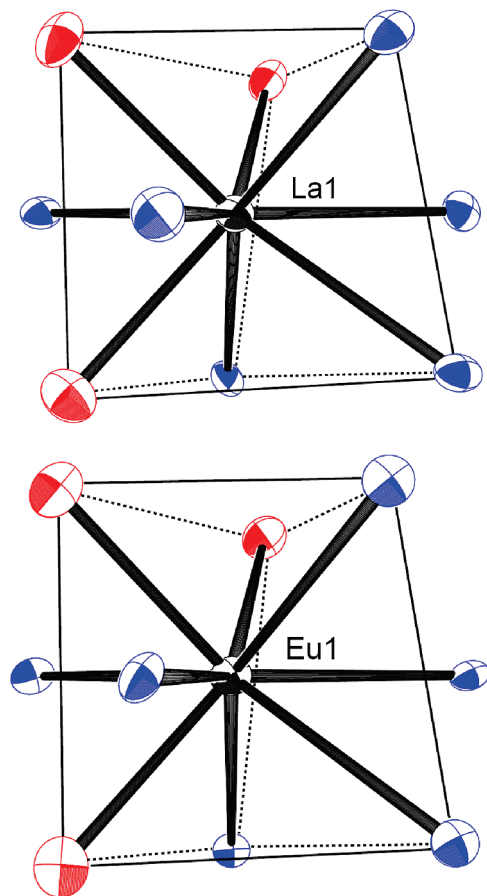


Figure 2. Coordination environments of Ln^{III} in $[\text{Ln}(\text{LPhBr})_3]$ ($\text{Ln} = \text{La}, \text{Eu}$) viewed down the square face of the tricapped trigonal prism. Heteroatoms: O, red; N, blue; Ln, black.

The relative bonding strengths of the ligands have been quantified with the bond-valence method³⁷ wherein a donor atom j at a distance $d_{\text{Ln},j}$ from the metal ion is characterized by a bond-valence contribution $\nu_{\text{Ln},j}$:

$$\nu_{\text{Ln},j} = e^{(R_{\text{Ln},j} - d_{\text{Ln},j})/b} \quad (1)$$

where $R_{\text{Ln},j}$ are the bond-valence parameters for the pair of interacting atoms ($\text{Ln}-\text{O}$ ³⁸ or $\text{Ln}-\text{N}$ ³⁹), and b is a constant equal to 0.37 Å. The bond valence sum (BVS) of the metal ion V_{Ln} defined by eq 2 is supposed to match its formal oxidation state if average bond distances are standard:

$$V_{\text{Ln}} = \sum_j \nu_{\text{Ln},j} \quad (2)$$

The BVS for LnLPhBr ($\text{Ln} = \text{La}, \text{Eu}$) and EuLPh ³⁰ are in the range 2.94–3.18, and match the expected value for Ln^{III} (3.00) within the variability of the method, accepted to be ± 0.25 valence units, and confirm the good quality of the crystallographic data (Table 2). The average contributions from the coordinating groups are in the expected

Table 2. Calculated Bond Valence Parameters^a

complex	V_{Ln}	$\nu_{\text{Ln},j}(\text{O})$	$\nu_{\text{Ln},j}(\text{N})$		
			N(py)	N(b)	N(av.)
$[\text{La}(\text{LPhBr})_3]$	3.18	0.45(5)	0.34(4)	0.27(5)	0.31(9)
$[\text{Eu}(\text{LPhBr})_3]$	3.06	0.42(6)	0.35(3)	0.26(4)	0.30(11)
$[\text{Eu}(\text{LPh})_3]^b$	2.94	0.40(8)	0.33(3)	0.26(10)	0.29(10)
all data		0.42(7)	0.34(4)	0.26(6)	0.30(9)

^aAveraged bond-valence contribution is listed with standard deviation (2σ) in parentheses. ^bFrom ref 30.

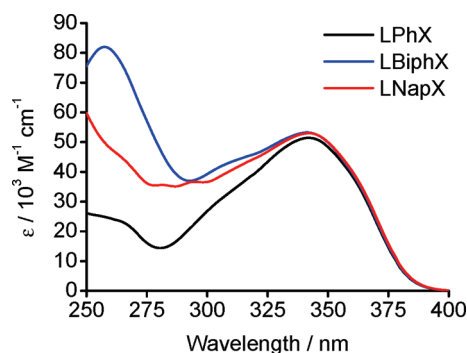


Figure 3. Absorption spectra of europium complexes $[\text{Eu}(\text{LRX})_3] \cdot n\text{H}_2\text{O}$ ($\text{R} = \text{Ph}, \text{Biph}, \text{Nap}$) at $(4.22\text{--}5.24) \times 10^{-5}$ M in CH_2Cl_2 . Additional absorption spectra are provided in the Supporting Information.

series, $\nu(\text{O}), 0.42(7) > \nu(\text{N-py}), 0.34(4) > \nu(\text{N-b}), 0.26(6)$ (Table 2), and similar to the ones previously reported for complexes with N -alkyl substituted ligands.³¹

Electronic States of the Ligands. UV–vis absorption spectra have been recorded in DMSO for the ligands, and in non-coordinating CH_2Cl_2 for the complexes (the ligands themselves are insoluble in CH_2Cl_2). Representative spectra for Eu^{III} complexes are shown in Figure 3 while spectra for all ligands and their complexes with La^{III} and Eu^{III} are displayed on Figures S1–S6 (Supporting Information). The main spectral features are presented in Table 3 and Table S1 (Supporting Information).

The ligands display a composite broad band in the UV corresponding to $\pi \rightarrow \pi^*$ transitions with a lowest-energy maximum at 303–324 nm and molar absorption coefficients of $(17\text{--}20) \times 10^3 \text{ M}^{-1}\text{cm}^{-1}$ assigned to the benzimidazole chromophore. Its position does not depend on the identity of N -aryl chromophore at benzimidazole indicating lack of electronic communication between the two aromatic moieties. Introduction of an electron-donor n -octyloxy group at the C(6)-atom of benzimidazole red-shifts this absorption by 20 nm which can be explained by a contribution of a benzimidazole-localized charge-transfer transition wherein the imine group acts as an acceptor. The variation of N -aryl from phenyl via naphthyl to biphenyl enhances the absorption of the ligand at 250–350 nm because of a contribution of the corresponding chromophore (Figure 3).

Upon complex formation, the lowest-energy band of the ligand is red-shifted by ≈ 20 nm, and its intensity increases to $(50\text{--}56) \times 10^3 \text{ M}^{-1}\text{cm}^{-1}$ reflecting the presence of three ligands in the complex. The trends in the absorption spectra of the complexes are identical to the ones observed for the free ligands.

(37) Brown, I. D.; Altermatt, D. *Acta Crystallogr., Sect. B* **1985**, *41*, 244.

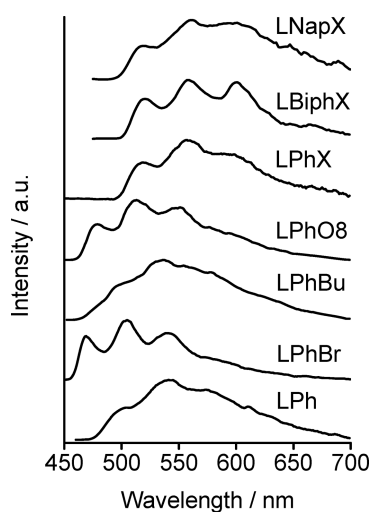
(38) Trzesowska, A.; Kruszynski, R.; Bartzak, T. J. *Acta Crystallogr., Sect. B* **2004**, *60*, 174.

(39) Trzesowska, A.; Kruszynski, R.; Bartzak, T. J. *Acta Crystallogr., Sect. B* **2005**, *61*, 429.

Table 3. Absorption Spectra of the Ligands in DMSO and of the Europium Complexes in CH₂Cl₂^a

	λ_{\max}/nm ($\epsilon/10^3 \text{ M}^{-1} \text{ cm}^{-1}$)		
HLPh	304 (18)	[Eu(LPh) ₃]·1.5H ₂ O ^b	322 (53)
HLPhBr	305 (18)	[Eu(LPhBr) ₃]·2.5H ₂ O ^b	321 (53)
HLPhBu·0.5H ₂ O	304 (17)	[Eu(LPhBu) ₃]·1.5H ₂ O	321 (53)
HLPhO8	303 (17)	[Eu(LPhO8) ₃]·2H ₂ O	322 (55)
HLPhX	325 (19)	[Eu(LPhX) ₃]·1.5H ₂ O	342 (51)
HLBiphX	324 (20)	[Eu(LBiphX) ₃]	342 (53)
	267 (27)		258 (82)
HLNapX	324 (20)	[Eu(LNapX) ₃]·H ₂ O	342 (53)
			295 (37)
			282 (36)

^aSpectra were recorded at room temperature in the range 250–500 nm. Estimated errors are ± 1 nm for λ_{\max} and $\pm 5\%$ for ϵ . Absorption data for La^{III} complexes are similar and are provided in Table S1 (Supporting Information). Concentration of Eu^{III} complexes was $(4.22\text{--}5.78) \times 10^{-5}$ M. ^bRecorded in DMSO. The complex is insoluble in CH₂Cl₂; its ϵ has been calculated by assuming that it remains undissociated in DMSO.

**Figure 4.** Phosphorescence spectra (corrected and normalized; emission slit: 5 nm) of lanthanum complexes in solid state at 77 K.

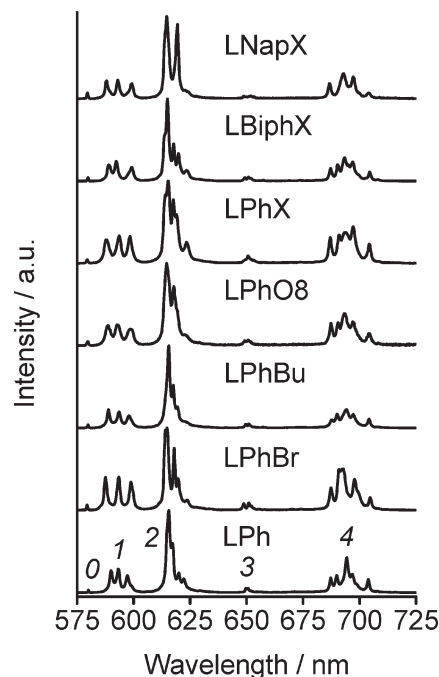
For a ligand to be a good sensitizer, its donor state, usually the first triplet state, should be situated sufficiently above the emitting ⁵D₀ level of Eu^{III} to allow efficient energy transfer to higher excited states of the metal and to prevent quenching by back energy transfer.^{11,12} The triplet energies of the ligands, E_T , have been determined to be $(19.2\text{--}21.3) \times 10^5 \text{ cm}^{-1}$ from the zero phonon transition in the phosphorescence spectra of the lanthanum complexes which display vibrational progression with a spacing of $(1.2\text{--}1.6) \times 10^3 \text{ cm}^{-1}$ attributable to ring-breathing modes (Figure 4, Table 4). Changing the 4-substituent on the *N*-phenyl ring results in variation of E_T within 1500 cm^{-1} in the series Br > OC₈H₁₇ > *tert*-butyl > H. Replacement of the C(6)-substituent in the benzimidazole ring from H to OC₈H₁₇ (LaLPh versus LaLPhX) lowers E_T by 500 cm^{-1} while variation of the *N*-aryl group in the LaLRX series (R = Ph, Biph, Nap) has no effect on E_T . Overall, the energy gap between E_T and ⁵D₀ states in the new complexes is in the range $1950\text{--}4050 \text{ cm}^{-1}$, which is suitable for sensitization of Eu^{III} luminescence.^{11,12}

Europium-Centered Luminescence. All new europium complexes emit characteristic metal-centered luminescence

Table 4. Energies of the Phonon Transitions in the Phosphorescence Spectra of Lanthanum Complexes in Solid State at 77 K^a

complex	$E/10^3 \text{ cm}^{-1}$		
	0→0	0→1	Δ
[La(LPh) ₃]·3H ₂ O	19.8	18.5	1.3
[La(LPhBr) ₃]·3H ₂ O	21.3	19.8	1.5
[La(LPhBu) ₃]·2H ₂ O	20.2	18.6	1.6
[La(LPhO8) ₃]·2H ₂ O	20.9	19.5	1.4
[La(LPhX) ₃]·2H ₂ O	19.3	18.0	1.3
[La(LBiphX) ₃]·H ₂ O	19.2	18.0	1.2
[La(LNapX) ₃]·H ₂ O	19.2	17.8	1.4

^aEstimated error on the energy is $\pm 200 \text{ cm}^{-1}$.

**Figure 5.** Luminescence spectra (corrected and normalized) of europium complexes in solid state at room temperature displaying the ⁵D₀→⁷F_J, J = 0–4, transitions; $\lambda_{\text{exc}} = 355 \text{ nm}$; emission slit: 0.2 nm.

in solid state and in CH₂Cl₂ (Figures 5 and 6). The corresponding excitation spectra display ligand bands below 425 nm which confirms sensitization of Eu^{III} emission by the ligands (Figure S7 in the Supporting Information).

In the solid state, the emission spectra consist of sharp bands due to ⁵D₀→⁷F_J transitions (denoted as 0→J) with their fine structure depending on the complex (Figure 5). For EuLPhBr, the 0→1 transition features three equally spaced components of similar intensity which is characteristic of Eu^{III} ion in a low symmetry environment and is in line with the results of crystal structure analysis; similar patterns are observed for EuLPhBu, EuLPhX, and EuLNapX. In contrast, the 0→1 transition for EuLPh,³⁰ EuLBiphX, and EuLPhO8 with two more closely spaced higher-energy components reflects a distorted pseudo-C₃ symmetry around the metal ion. In solution, the spectra are broader and are nearly identical for all the complexes (Figure 6), with the splitting pattern of the 0→1 transition pointing to Eu^{III} environments derived from a distorted pseudo-C₃ symmetry. Luminescence spectra in all media are independent of excitation wavelength. The emission

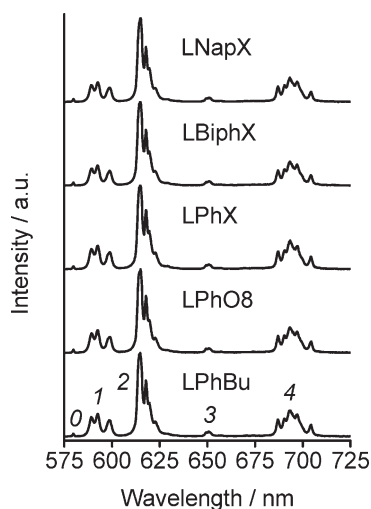


Figure 6. Luminescence spectra (corrected and normalized) of europium complexes in $(5.86\text{--}7.75) \times 10^{-4}$ M solution in CH_2Cl_2 at room temperature displaying the $^5\text{D}_0 \rightarrow ^7\text{F}_J$, $J = 0\text{--}4$, transitions; $\lambda_{\text{exc}} = 355$ nm; emission slit: 0.2 nm.

intensity is fairly equally distributed in the range 575–720 nm with the hypersensitive $0 \rightarrow 2$ transition dominating the spectrum. The $0 \rightarrow 0$ and $0 \rightarrow 3$ transitions are weak, representing $<0.6\%$ and $<3\%$ of the total emission, respectively (Table S2 in the Supporting Information). The contributions of the $0 \rightarrow 1$, $0 \rightarrow 2$, and $0 \rightarrow 4$ transitions to the total emission are nearly constant in solution, with averages of 17(1), 50(2), and 30(1)%, respectively; in the solid state, these values display larger variation being equal to 19(3), 46(8), and 32(5)%, respectively (Table S2 in the Supporting Information).

The emission of europium complexes can be analyzed in terms of eq 3 where Q_{L}^{Eu} and $Q_{\text{Eu}}^{\text{Eu}}$ are ligand-sensitized and intrinsic luminescence quantum yields of Eu^{III} ; η_{sens} is the efficiency of the ligand-to-metal energy transfer; τ_{obs} and τ_{rad} are the observed and radiative lifetimes of $\text{Eu}(^5\text{D}_0)$:

$$Q_{\text{L}}^{\text{Eu}} = \eta_{\text{sens}} \times Q_{\text{Eu}}^{\text{Eu}} = \eta_{\text{sens}} \times (\tau_{\text{obs}}/\tau_{\text{rad}}) \quad (3)$$

To achieve bright luminescence, the ligands must protect Eu^{III} from non-radiative deactivation (term $Q_{\text{Eu}}^{\text{Eu}}$), and provide efficient light harvesting and energy transfer (term η_{sens}).

The observed luminescence decays (τ_{obs}) are single exponential functions for all europium complexes in all media at 298 and 10 K indicating the presence of only one emissive Eu^{III} center. They are long, 1.8–2.6 ms in solid state and 2.2–2.7 ms in solution and vary by less than 20% in solid state between 298 and 10 K which points to the absence of significant thermally activated deactivation pathways (Table 5, Table S3 in the Supporting Information). They are consistent with the absence of water in the inner coordination sphere of europium and suggest that the metal ion is well shielded from non-radiative deactivation by the ligands.

The quantum yields of ligand-sensitized europium luminescence (Q_{L}^{Eu}) are large: 43–59% in solid state and 38–49% in CH_2Cl_2 (Table 5) and are independent of λ_{exc} within experimental error (Table S3 in the Supporting Information).

The intrinsic quantum yields of europium could not be determined experimentally upon direct f-f excitation because of very low absorption intensity. Therefore, radiative lifetimes of $\text{Eu}(^5\text{D}_0)$ have been calculated from eq 4,⁴⁰ where n is the refractive index (1.5 for solid state metal-organic complexes; 1.4242 for CH_2Cl_2), $A_{\text{MD},0}$ is the spontaneous emission probability for the $^5\text{D}_0 \rightarrow ^7\text{F}_1$ transition in vacuo (14.65 s^{-1}), and $I_{\text{tot}}/I_{\text{MD}}$ is the ratio of the total integrated intensity of the corrected Eu^{III} emission spectrum to the integrated intensity of the magnetic dipole $^5\text{D}_0 \rightarrow ^7\text{F}_1$ transition (Table S2 in the Supporting Information):

$$1/\tau_{\text{rad}} = A_{\text{MD},0} \times n^3 \times (I_{\text{tot}}/I_{\text{MD}}) \quad (4)$$

The calculated radiative lifetimes are long: 3.2–4.3 ms in solid state, increasing to 3.9–4.2 ms in CH_2Cl_2 (Table 5). The intrinsic quantum yields of europium estimated from the ratio $\tau_{\text{obs}}/\tau_{\text{rad}}$ are high: 49–65% in all media (Table 5). The relatively small variations of τ_{rad} and $Q_{\text{Eu}}^{\text{Eu}}$ are an outcome of the similar N_6O_3 -coordination environment for all the complexes.

The sensitization efficiencies calculated from the ratio $Q_{\text{L}}^{\text{Eu}}/Q_{\text{Eu}}^{\text{Eu}}$ are nearly quantitative ($>90\%$) in solid state, except for **EuLNapX** (77%) (Table 5). In solution, they become smaller, 70–80%, which probably reflects energy losses within the ligands by collisional deactivation with solvent molecules and via labile ligand-lanthanide bonding; as a result, Q_{L}^{Eu} is lower in solution compared to solid state samples.

Conclusions

We have developed a facile approach to *N*-aryl chromophore substituted benzimidazole pyridine-2-carboxylic acids. Despite steric hindrance, these ligands form 9-coordinate lanthanide complexes $[\text{Ln}(\text{Ligand})_3] \cdot n\text{H}_2\text{O}$. The europium complexes are highly luminescent in solid state and in solution with ligand-sensitized quantum yields and observed lifetimes reaching 59% and 2.7 ms, respectively, and ligand-to- Eu^{III} energy-transfer efficiencies exceeding 70%.

The sensitized quantum yields of europium complexes, Q_{L}^{Eu} , decrease as the energy gap between the ligand triplet state and the emissive $^5\text{D}_0$ level of Eu^{III} becomes smaller (Figure 7) which facilitates quenching by back energy transfer from metal to ligand.^{11,12} The correlation is applicable to both the *N*-aryl complexes and to the previously reported³¹ *N*-alkyl complexes with the optimum energy gap being $>2000 \text{ cm}^{-1}$ ($E_{\text{T}} > 19300 \text{ cm}^{-1}$), providing $Q_{\text{L}}^{\text{Eu}} > 50\%$. For the “solution data”, the correlation is smooth, reflecting only the variation of E_{T} . The relatively large scattering of the “solid state data” in Figure 7 is likely to reflect the effect of second sphere quenching of Eu^{III} by co-crystallized water:

- (i) In the complexes containing co-crystallized water, τ_{obs} increases by up to 25% when going from the solid state to CH_2Cl_2 while τ_{obs} of the anhydrous complex **EuLBiphX** is nearly independent of the medium (Table 5). We suggest that co-crystallized water in the former compounds contributes to the quenching of the emissive state of Eu^{III} via

(40) Werts, M. H. V.; Jukes, R. T. F.; Verhoeven, J. W. *Phys. Chem. Chem. Phys.* **2002**, *4*, 1542.

Table 5. Photophysical Properties of Eu^{III} Complexes^a

complex		$Q_L^{\text{Eu}}/\%$	$\tau_{\text{obs}}/\text{ms}^b$		$\tau_{\text{rad}}/\text{ms}$	$Q_{\text{Eu}}^{\text{Eu}}/\%$	$\eta_{\text{sens}}/\%$
			298 K	10 K			
[Eu(LPh) ₃]·1.5H ₂ O	solid	54(2)	2.02(1)	2.12(2)	4.12	49	≈100
[Eu(LPhBr) ₃]·2.5H ₂ O	solid	59(2)	2.64(3)	2.58(2)	4.28	62	95(14)
[Eu(LPhBu) ₃]·1.5H ₂ O	solid	57(2)	2.19(1)	2.23(2)	3.87	57	100(15)
	CH ₂ Cl ₂	49(3)	2.70(3)		4.19	64	77(12)
[Eu(LPhO8) ₃]·2H ₂ O	solid	57(2)	2.24(1)	2.32(1)	3.84	58	98(15)
	CH ₂ Cl ₂	47(1)	2.76(1)		4.22	65	72(11)
[Eu(LPhX) ₃]·1.5H ₂ O	solid	46(2)	2.02(2)	2.39(1)	3.95	51	90(14)
	CH ₂ Cl ₂	40(1)	2.51(4)		4.19	60	67(10)
[Eu(LBiphX) ₃]	solid	58(2)	2.24(2)	2.25(1)	3.64	62	94(14)
	CH ₂ Cl ₂	42(1)	2.36(1)		3.92	60	70(11)
[Eu(LNapX) ₃]·H ₂ O	solid	43(2)	1.84(2)	2.06(2)	3.22	57	77(12)
	CH ₂ Cl ₂	38(1)	2.24(2)		3.91	57	67(10)

^a At 298 K, unless stated otherwise. In solid state or $(5.86-7.75) \times 10^{-4}$ M in CH₂Cl₂ at $\lambda_{\text{exc}} = 355$ nm. Standard deviations (2σ) are given between parentheses; estimated relative errors: τ_{obs} , ±2%; Q_L^{Eu} , ±10%; τ_{rad} , ±10%; $Q_{\text{Eu}}^{\text{Eu}}$, ±12%; η_{sens} , ±22%. Photophysical parameters at other excitation wavelengths are collected in Table S3 in the Supporting Information. ^b In solid state, τ_{obs} may show variation by ≈10% when λ_{exc} is changed between 320 and 527 nm; in CH₂Cl₂, τ_{obs} are independent of λ_{exc} (Table S3 in the Supporting Information).

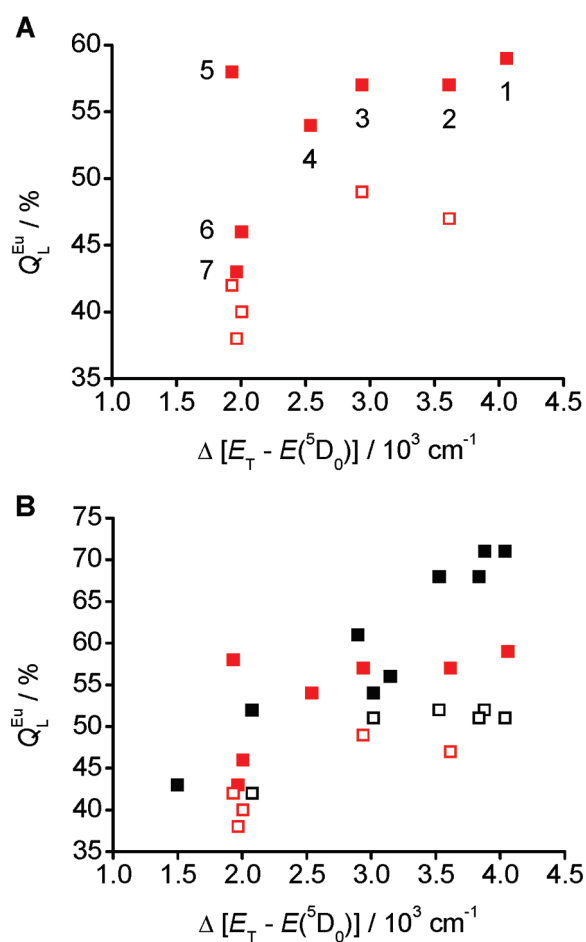


Figure 7. Dependence of the sensitized luminescence quantum yield of Eu^{III} on the energy gap between the triplet state of the ligand (zero phonon) and Eu^{III}(⁵D₀ = 17260 cm⁻¹) state in the solid (■) and in CH₂Cl₂ solution (□) at room temperature. **A:** *N*-Aryl complexes; 1: **EuLPhBr**; 2: **EuLPhO8**; 3: **EuLPhBu**; 4: **EuLPh**; 5: **EuLBiphX**; 6: **EuLPhX**; 7: **EuLNapX**. **B:** *N*-Aryl complexes (in red) are presented together with the previously reported³¹ *N*-alkyl complexes (in black).

second-sphere interaction in the solid state, while in CH₂Cl₂, water dissociates, which eliminates quenching and increases τ_{obs} .⁴¹

- (ii) In solid state, the anhydrous complex **EuLBiphX** displays a higher Q_L^{Eu} compared to the “hydrated”

complexes with similar E_T , that is, **EuLPhX** and **EuLNapX**. On the other hand, these three complexes have comparable Q_L^{Eu} in CH₂Cl₂, again because of the dissociation of co-crystallized water (Table 5, Figure 7A).⁴¹

- (iii) The *N*-aryl complexes **EuLPhBr** and **EuLPhO8** containing 2–2.5 co-crystallized water molecules display lower $Q_L^{\text{Eu}} = 57-59\%$ compared to $Q_L^{\text{Eu}} = 68-71\%$ for the “anhydrous” *N*-alkyl complexes³¹ with similar E_T (Figure 7B).

With regard to the influence of ligand structure on the luminescence efficiency of europium we notice that the introduction of a *para*-substituent at the *N*-phenyl ring in going from H (**EuLPh**) to Br (**EuLPhBr**), *tert*-butyl (**EuLPhBu**) or OC₈H₁₇ (**EuLPhO8**) has no effect on Q_L^{Eu} even though the triplet states of the corresponding ligands vary up to 1500 cm⁻¹. In contrast, the grafting of a OC₈H₁₇ substituent on the C(6) atom of benzimidazole lowers Q_L^{Eu} from 54% (**EuLPh**) to 46% (**EuLPhX**) reflecting a small decrease in E_T by 500 cm⁻¹. Therefore, synthetic modification of the ligands at the *N*-aryl group might be preferred to that at benzimidazole, as it appears to have less negative influence on the luminescence of europium. In fact, even the variation of the *N*-aryl group in the **EuLRX** series with R = Ph, Nap, Biph, has little influence on Q_L^{Eu} ; however, this trend is likely to change for *N*-aryl chromophores with lower energies of electronic states compared to that of benzimidazole.

Therefore, the replacement of the *N*-alkyl substituent³¹ at benzimidazole with *N*-aryl (aryl = phenyl, 4-biphenyl, 2-naphthyl) provides enhanced absorption to the lanthanide complexes, but it does not significantly alter either their structural parameters, or the intrinsic photophysical properties of europium (τ_{rad} and $Q_{\text{Eu}}^{\text{Eu}}$), or the ligand-to-metal energy transfer efficiency. This study demonstrates the amenability of tridentate benzimidazole-pyridine 2-carboxylates to modification, and points to these ligands as promising candidates for the development of brightly emissive europium compounds for display and lighting applications.

(41) Shavaleev, N. M.; Scopelliti, R.; Gummy, F.; Bünzli, J.-C. G. *Inorg. Chem.* **2009**, *48*, 7937.

Table 6. Crystal Data and Structure Refinement^a

	[La(LPhBr) ₃]	[Eu(LPhBr) ₃]
empirical formula	C ₅₇ H ₃₃ Br ₃ LaN ₉ O ₆ ·4C ₂ H ₅ OH·3H ₂ O	C ₅₇ H ₃₃ Br ₃ EuN ₉ O ₆ ·4C ₂ H ₅ OH·3H ₂ O
fw	1556.88	1569.93
cryst syst	triclinic	triclinic
space group	<i>P</i> $\bar{1}$	<i>P</i> $\bar{1}$
unit cell dimensions	<i>a</i> = 12.3326(7) Å <i>b</i> = 15.8747(9) Å <i>c</i> = 17.8434(11) Å α = 71.845(5)° β = 75.155(5)° γ = 89.695(5)°	<i>a</i> = 12.2911(6) Å <i>b</i> = 15.8191(7) Å <i>c</i> = 17.5508(8) Å α = 72.415(4)° β = 75.272(4)° γ = 89.408(4)°
vol [Å ³]	3198.0(3)	3137.9(3)
<i>Z</i>	2	2
ρ (calc) [Mg/m ³]	1.617	1.662
μ [mm ⁻¹]	2.613	2.982
<i>F</i> (000)	1564	1576
cryst size [mm ³]	0.34 × 0.30 × 0.25	0.28 × 0.20 × 0.13
θ range	2.99 – 27.48°	2.99 – 26.02°
index ranges	–16 ≤ <i>h</i> ≤ 16 –19 ≤ <i>k</i> ≤ 20 –22 ≤ <i>l</i> ≤ 23	–14 ≤ <i>h</i> ≤ 15 –19 ≤ <i>k</i> ≤ 19 –21 ≤ <i>l</i> ≤ 18
reflns collected	14575	24585
independent reflns	14575 [<i>R</i> (int) = 0.0000]	12322 [<i>R</i> (int) = 0.0444]
completeness to θ	27.48° – 99.3%	26.02° – 99.6%
max/min transm	1.00000/0.76643	1.00000/0.51159
data/restraints/params	14575/48/822	12322/66/820
GOF on <i>F</i> ²	1.036	0.977
final <i>R</i> indices [<i>I</i> > 2 σ (<i>I</i>)]	<i>R</i> 1 = 0.0646 <i>wR</i> 2 = 0.1509	<i>R</i> 1 = 0.0560 <i>wR</i> 2 = 0.1399
<i>R</i> indices (all data)	<i>R</i> 1 = 0.1149 <i>wR</i> 2 = 0.1674	<i>R</i> 1 = 0.0810 <i>wR</i> 2 = 0.1482
largest diff. peak/hole [e/Å ³]	2.142/–1.099	2.974/–1.708

^aData in common: Temperature, 140(2) K. Wavelength, 0.71073 Å. Refinement method, full-matrix least-squares on *F*². Absorption correction: semiempirical from equivalents.

Experimental Section

General Methods, Equipment, and Chemicals Used. Elemental analyses were performed by Dr. E. Solari, Service for Elemental Analysis, Institute of Chemical Sciences and Engineering (EPFL). ¹H and ¹³C NMR spectra (presented as δ in ppm and *J* in Hz) were recorded on a Bruker Avance DRX 400 MHz and Bruker Avance II 800 MHz spectrometers, respectively. ESI MS were recorded on a Q-TOF Ultima (Waters) or TSQ7000 (Thermo Fisher) spectrometers at the Mass Spectrometry Service of the Institute of Chemical Sciences and Engineering (EPFL). Absorption spectra were measured on a Perkin-Elmer Lambda 900 UV/vis/NIR spectrometer at room temperature in the spectral range 250–500 nm. Estimated errors are ± 1 nm for λ_{max} and $\pm 5\%$ for ϵ . Luminescence spectra were measured on a Fluorolog FL 3-22 spectrometer from Horiba-Jobin Yvon and were corrected for the instrumental function. Quantum yields were determined on the same instrument through an absolute method using a home-modified integrating sphere.⁴² Luminescence lifetimes were measured with a previously described instrumental setup.³¹ Spectroscopic studies were conducted in optical cells of 2 mm path length or 2 mm i.d. quartz capillaries under air with the samples of lanthanide complexes obtained directly from the synthesis and used without further purification. The solutions of the complexes in CH₂Cl₂ (Fisher Scientific, analytical reagent grade) were freshly prepared before each experiment.

X-ray Crystallography. The crystal data and structure refinement parameters are presented in Table 6. Single crystals were grown by dissolving a small sample (1–2 mg) of the complex in boiling C₂H₅OH for [La(LPhBr)₃] or C₂H₅OH/CH₃CN for [Eu(LPhBr)₃] followed by cooling to room temp. and slow evaporation (1–4 weeks).

Data collections for both structures were performed at 140 K using Mo *K* α radiation on an Oxford Diffraction Sapphire/KM4 CCD with a kappa geometry goniometer. Data were reduced by means of CrysAlis PRO⁴³ and then corrected for absorption.⁴⁴ Solutions and refinements were carried by SHELX.⁴⁵ The structures were refined using full-matrix least-squares on *F*² with all non hydrogen atoms anisotropically defined. Hydrogen atoms were placed in calculated positions by means of the “riding” model (apart from the ones belonging to water molecules).

Solvent molecules in both structures were clearly disordered; however, disorder was not modeled and restraints (SIMU and ISOR cards) were applied to displacement parameters of the C₂H₅OH and H₂O molecules. A twinning problem was discovered during the refinement of [La(LPhBr)₃] and treated by means of the TWINROT routine in PLATON.⁴⁶ A new data set was then created and used in the final stages of refinement with cards HKLF 5, MERG 0, and two refined BASF parameters [0.096(1); 0.080(4)].

Synthesis of Benzimidazole-Substituted Pyridine-2-Carboxylic Acids. The synthesis of the precursors is described in the Supporting Information. The reactions were performed under air. Substituted pyridine-2-carboxaldehyde was dissolved in formic acid (Merck, 98–100%) at room temp. to give a yellow solution which sometimes appeared as being cloudy because of the presence of a red solid, probably, residual Se from the previous synthetic step. The amount of formic acid was chosen to correspond either to a minimum of 3–5 mol equiv relative to aldehyde or to the minimum volume necessary to dissolve the aldehyde at 0 °C.

(43) CrysAlis PRO; Oxford Diffraction Ltd.: Yarnton, Oxfordshire, U.K., 2009.

(44) Blessing, R. H. *Acta Crystallogr., Sect. A* **1995**, *51*, 33.

(45) Sheldrick, G. *Acta Crystallogr., Sect. A* **2008**, *64*, 112.

(46) Spek, A. L. *PLATON. A Multipurpose Crystallographic Tool*; Utrecht University: Utrecht, The Netherlands, 2008.

(42) Aebischer, A.; Gummy, F.; Bünzli, J.-C. G. *Phys. Chem. Chem. Phys.* **2009**, *11*, 1346.

This solution was cooled to 0 °C, stirred for 10 min, and cold H₂O₂ (30% wt. aq. solution) was added in excess. The solution was stirred at 0 °C for 4–6 h, and kept overnight at 0 °C. Addition of ice-cold water (20 mL) precipitated the product. In the case of HLPPhO8 and HLRX (R = Ph, Biph, Nap) the product separates as sticky oil which solidifies on stirring and sonication. The resulting suspension was stirred at 0 °C for 1 h and filtered to give a solid. It was washed with water, ether (25 mL), and hexane for HLPPhBr or with water and hexane in all other cases, and was dried under vacuum. Synthesis of HLPPh has been described elsewhere.³⁰ Further specific synthetic details are provided below.

HLPPhBr. The reaction was performed with LPhBr-CHO (269 mg, 0.71 mmol), formic acid (4 mL, 4.88 g, 0.11 mol), and H₂O₂ (0.45 mL of 30% wt. aq. solution, containing 150 mg of H₂O₂, 4.41 mmol). White solid: 216 mg (0.55 mmol, 77%). Anal. Calcd for C₁₉H₁₂BrN₃O₂ (MW 394.22): C, 57.89; H, 3.07; N, 10.66. Found: C, 57.63; H, 3.07; N, 10.44. ¹H NMR (400 MHz, DMSO-*d*₆): 8.35 (d, *J* 7.2, 1H), 8.11 (t, *J* 7.6, 1H), 8.00 (d, *J* 7.6, 1H), 7.85 (dd, *J* 6.8, *J* 2.0, 1H), 7.71–7.65 (m, 2H), 7.42–7.31 (m, 4H), 7.23 (dd, *J* 6.8, *J* 2.0, 1H), CO₂H proton not observed. ¹³C NMR (200 MHz, DMSO-*d*₆): 165.97, 149.75, 149.00, 148.09, 142.66, 139.01, 137.67, 136.84, 132.61, 130.10, 127.71, 125.29, 124.82, 123.70, 121.64, 120.39, 111.37. ESI⁺ MS: *m/z* 394.1, 396.1 {M + H}⁺.

HLPPhBu. The reaction was performed with LPhBu-CHO (366 mg, 1.03 mmol), formic acid (4 mL, 4.9 g, 0.11 mol), and H₂O₂ (0.55 mL of 30% wt. aq. solution, containing 183 mg of H₂O₂, 5.39 mmol). White solid: 337 mg (0.91 mmol, 88%). Anal. Calcd for C₂₃H₂₁N₃O₂·0.5H₂O (MW 380.44): C, 72.61; H, 5.83; N, 11.05. Found: C, 72.44; H, 5.88; N, 10.86. ¹H NMR (400 MHz, DMSO-*d*₆): 8.29 (d, *J* 7.6, 1H), 8.09 (t, *J* 7.6, 1H), 7.99 (d, *J* 7.6, 1H), 7.85 (dd, 1H), 7.51 (d, *J* 8.4, 2H), 7.39–7.29 (m, 4H), 7.23 (dd, 1H), 1.33 (s, 9H), CO₂H proton not observed. ¹³C NMR (200 MHz, DMSO-*d*₆): 165.87, 151.19, 149.91, 149.20, 147.96, 142.61, 138.97, 137.78, 134.60, 127.92, 127.32, 126.47, 125.09, 124.64, 123.50, 120.32, 111.52, 34.95, 31.56. ESI⁺ MS: *m/z* 372.7 {M + H}⁺.

HLPPhO8. The reaction was performed with LPhO8-CHO (432 mg, 1.01 mmol), formic acid (4 mL, 4.9 g, 0.11 mol), and H₂O₂ (0.52 mL of 30% wt. aq. solution, containing 173 mg of H₂O₂, 5.09 mmol). White solid: 295 mg (0.67 mmol, 66%). Anal. Calcd for C₂₇H₂₉N₃O₃ (MW 443.54): C, 73.11; H, 6.59; N, 9.47. Found: C, 72.86; H, 6.72; N, 9.35. ¹H NMR (400 MHz, DMSO-*d*₆): 8.24 (d, *J* 7.6, 1H), 8.09 (t, *J* 7.6, 1H), 8.01 (d, *J* 7.6, 1H), 7.83 (dd, 1H), 7.39–7.28 (m, 4H), 7.19 (dd, 1H), 7.01 (d, *J* 8.8, 2H), 4.00 (t, *J* 6.8, 2H), 1.79–1.68 (m, 2H), 1.48–1.22 (m, 10H), 0.87 (t, *J* 6.8, 3H), CO₂H proton not observed. ¹³C NMR (200 MHz, DMSO-*d*₆): 165.98, 158.81, 150.22, 149.33, 148.11, 142.55, 138.88, 138.08, 129.60, 129.15, 128.00, 125.06, 124.51, 123.42, 120.28, 115.34, 111.45, 68.25, 31.73, 29.25, 29.16 (two overlapping resonances), 26.01, 22.58, 14.45. ESI⁺ MS: *m/z* 444.7 {M + H}⁺.

HLPPhX. The reaction was performed with LPhX-CHO (203 mg, 0.47 mmol), formic acid (3 mL, 3.66 g, 0.08 mol) and H₂O₂ (0.3 mL of 30% wt. aq. solution, containing 100 mg of H₂O₂, 2.93 mmol). Cream solid: 71 mg (0.16 mmol, 34%). Anal. Calcd for C₂₇H₂₉N₃O₃ (MW 443.54): C, 73.11; H, 6.59; N, 9.47. Found: C, 73.17; H, 6.62; N, 9.40. ¹H NMR (400 MHz, DMSO-*d*₆): 8.20–8.13 (br, 1H), 8.03 (t, *J* 7.6, 1H), 7.94 (d, *J* 8.0, 1H), 7.72 (d, *J* 8.8, 1H), 7.54–7.36 (m, 5H), 6.97 (dd, *J* 8.8, *J* 2.4, 1H), 6.60 (d, *J* 2.4, 1H), 3.91 (t, *J* 6.4, 2H), 1.73–1.63 (m, 2H), 1.43–1.20 (m, 10H), 0.85 (t, *J* 7.2, 3H), CO₂H proton not observed. ¹³C NMR (200 MHz, DMSO-*d*₆): 165.96, 157.11, 149.22, 148.24, 138.80, 138.46, 137.36, 137.03, 129.80, 128.68, 127.80, 127.43, 124.72, 121.05, 113.71, 94.68, 68.41, 31.68, 29.21, 29.15, 29.11, 25.98, 22.55, 14.43, one of the aromatic carbons is not observed. ESI⁺ MS: *m/z* 444.7 {M + H}⁺.

HLBiphX. The reaction was performed with LBiphX-CHO (376 mg, 0.75 mmol), formic acid (4 mL, 4.88 g, 0.11 mol), and

H₂O₂ (0.45 mL of 30% wt. aq. solution, containing 150 mg of H₂O₂, 4.41 mmol). Off-white solid: 239 mg (0.46 mmol, 61%). Anal. Calcd for C₃₃H₃₃N₃O₃ (MW 519.63): C, 76.28; H, 6.40; N, 8.09. Found: C, 76.53; H, 6.35; N, 8.24. ¹H NMR (400 MHz, DMSO-*d*₆): 8.28 (d, *J* 7.6, 1H), 8.08 (t, *J* 7.6, 1H), 7.96 (d, *J* 8.0, 1H), 7.82–7.70 (m, 5H), 7.55–7.46 (m, 4H), 7.41 (t, *J* 7.6, 1H), 6.99 (dd, *J* 8.8, *J* 2.4, 1H), 6.68 (d, *J* 2.0, 1H), 3.93 (t, *J* 6.4, 2H), 1.73–1.64 (m, 2H), 1.44–1.17 (m, 10H), 0.83 (t, *J* 7.2, 3H), CO₂H proton not observed. ¹³C NMR (200 MHz, DMSO-*d*₆): 165.94, 157.19, 149.28, 149.06, 147.91, 140.30, 139.81, 138.89, 138.52, 137.07, 136.73, 129.45, 128.35, 128.20, 127.92, 127.45, 127.31, 124.80, 121.08, 113.79, 94.75, 68.45, 31.68, 29.22, 29.16, 29.11, 25.98, 22.54, 14.41. ESI⁺ MS: *m/z* 520.7 {M + H}⁺.

HLNapX. The reaction was performed with LNapX-CHO (520 mg, 1.09 mmol), formic acid (5 mL, 6.1 g, 0.13 mol), and H₂O₂ (0.75 mL of 30% wt. aq. solution, containing 250 mg of H₂O₂, 7.34 mmol). Dull yellow solid: 246 mg (0.50 mmol, 46%, non-optimized yield). Anal. Calcd for C₃₁H₃₁N₃O₃ (MW 493.60): C, 75.43; H, 6.33; N, 8.51. Found: C, 75.44; H, 6.28; N, 8.55. ¹H NMR (400 MHz, DMSO-*d*₆): 8.28 (dd, *J* 8.0, *J* 0.8, 1H), 8.09–7.96 (m, 4H), 7.95 (dd, *J* 7.2, *J* 1.6, 1H), 7.91 (dd, *J* 7.6, *J* 0.8, 1H), 7.74 (d, *J* 8.8, 1H), 7.61–7.52 (m, 2H), 7.47 (dd, *J* 8.8, *J* 2.0, 1H), 6.97 (dd, *J* 8.8, *J* 2.4, 1H), 6.63 (d, *J* 2.4, 1H), 3.87 (t, *J* 6.4, 2H), 1.69–1.58 (m, 2H), 1.38–1.12 (m, 10H), 0.81 (t, *J* 6.8, 3H), CO₂H proton not observed. ¹³C NMR (200 MHz, DMSO-*d*₆): 165.78, 157.18, 149.29, 147.91, 138.86, 138.75, 137.07, 134.93, 133.53, 132.77, 129.47, 128.61, 128.19, 127.48, 127.13, 127.04, 126.28, 126.15, 124.80, 121.08, 113.80, 94.82, 68.39, 31.65, 29.19, 29.11, 29.08, 25.95, 22.52, 14.39, one of the aromatic carbons is not observed. ESI⁺ MS: *m/z* 494.7 {M + H}⁺.

Synthesis of the Complexes. The reactions were performed under air using 3:3:1 molar ratio of the ligand, NaOH, and LnCl₃·*n*H₂O. The ligand was suspended in hot ethanol (70–80 °C, 5 mL; the same temperature was kept throughout the reaction), followed by addition of NaOH dissolved in water (0.5–1 mL, used as a stock solution with approximately 100 mg of NaOH per 10 mL of water) and stirring for 10 min to give colorless solution. A solution of LnCl₃·*n*H₂O (*n* = 6 or 7; 99.9%, Aldrich) in water (2 mL) was added dropwise over 5 min and stirred for further 5 min. A white precipitate of the complex may form on addition. If necessary, an additional volume of water (as specified below) was added to complete the precipitation of the complex. The resulting suspension was stirred for 5 min at 70–80 °C, allowed to cool to 40–50 °C while stirring, and filtered while warm. The product was washed with ethanol/water (1:1) followed by ether for LnLPhBr; with ethanol/water (1:4) and hexane for LnLPhBu; or with ethanol/water (1:1) followed by hexane in all other cases, and was dried under vacuum at room temperature. The complexes are white solids that are soluble in DMSO, boiling ethanol and are insoluble in hexane and water; the complexes with *tert*-butyl or *n*-octyloxy groups are also soluble in CH₂Cl₂. Further synthetic details and analytical data are provided below. Synthesis of LnLPh has been described elsewhere.³⁰

[La(LPhBr)₃]·3H₂O. The complex precipitated on mixing of reagents: 48 mg (0.035 mmol, 83%) from HLPPhBr (50 mg, 0.127 mmol), NaOH (5.1 mg, 0.127 mmol), and LaCl₃·7H₂O (15.7 mg, 0.042 mmol). Anal. Calcd for C₅₇H₃₃Br₃LaN₉O₆·3H₂O (MW 1372.59): C, 49.88; H, 2.86; N, 9.18. Found: C, 50.14; H, 2.81; N, 8.72. ESI⁺ MS: *m/z* 1342.4 {M + Na}⁺, 682.7 {M + 2Na}²⁺.

[La(LPhBu)₃]·2H₂O. The complex was precipitated with water (8 mL): 45 mg (0.035 mmol, 80%) from HLPPhBu·0.5H₂O (50 mg, 0.131 mmol), NaOH (5.25 mg, 0.131 mmol), and LaCl₃·7H₂O (16.3 mg, 0.044 mmol). Anal. Calcd for C₆₉H₆₀LaN₉O₆·2H₂O (MW 1286.21): C, 64.43; H, 5.02; N, 9.80. Found: C, 64.26; H, 4.93; N, 9.77. ESI⁺ MS: *m/z* 1250.8 {M + H}⁺, 625.9 {M + 2H}²⁺.

[La(LPhO8)₃]·2H₂O. The complex was precipitated with water (2.5 mL): 43 mg (0.029 mmol, 75%) from HLPPhO8 (50 mg,

0.113 mmol), NaOH (4.51 mg, 0.113 mmol), and $\text{LaCl}_3 \cdot 7\text{H}_2\text{O}$ (13.95 mg, 0.038 mmol). Anal. Calcd for $\text{C}_{81}\text{H}_{84}\text{LaN}_9\text{O}_9 \cdot 2\text{H}_2\text{O}$ (MW 1502.52): C, 64.75; H, 5.90; N, 8.39. Found: C, 64.84; H, 5.96; N, 8.26. ESI⁺ MS: m/z 756.0 {M + 2Na}²⁺.

[La(LPhX)₃·2H₂O]. The complex was precipitated with water (1 mL): 25 mg (0.017 mmol, 88%) from HLPPhX (25 mg, 0.056 mmol), NaOH (2.25 mg, 0.056 mmol), and $\text{LaCl}_3 \cdot 7\text{H}_2\text{O}$ (7.0 mg, 0.019 mmol). Anal. Calcd for $\text{C}_{81}\text{H}_{84}\text{LaN}_9\text{O}_9 \cdot 2\text{H}_2\text{O}$ (MW 1502.52): C, 64.75; H, 5.90; N, 8.39. Found: C, 64.64; H, 5.92; N, 8.23. ESI⁺ MS: m/z 756.1 {M + 2Na}²⁺. ¹H NMR (400 MHz, CD₂Cl₂) of the complex indicates the presence of several interconverting species in solution (Figure NMR-25 in the Supporting Information).

[La(LBiphX)₃·H₂O]. The complex precipitated on mixing of reagents: 47 mg (0.029 mmol, 91%) from HLBiphX (50 mg, 0.096 mmol), NaOH (3.85 mg, 0.096 mmol), and $\text{LaCl}_3 \cdot 7\text{H}_2\text{O}$ (11.9 mg, 0.032 mmol). Anal. Calcd for $\text{C}_{99}\text{H}_{96}\text{LaN}_9\text{O}_9 \cdot \text{H}_2\text{O}$ (MW 1712.80): C, 69.42; H, 5.77; N, 7.36. Found: C, 69.27; H, 5.73; N, 7.35. ESI⁺ MS: m/z 870.6 {M + 2Na}²⁺.

[Eu(LNapX)₃·H₂O]. The complex was precipitated with water (1 mL): 46 mg (0.28 mmol, 83%) from HLNapX (50 mg, 0.10 mmol), NaOH (4.05 mg, 0.10 mmol), and $\text{LaCl}_3 \cdot 7\text{H}_2\text{O}$ (12.5 mg, 0.034 mmol). Anal. Calcd for $\text{C}_{93}\text{H}_{90}\text{LaN}_9\text{O}_9 \cdot \text{H}_2\text{O}$ (MW 1634.69): C, 68.33; H, 5.67; N, 7.71. Found: C, 68.07; H, 5.75; N, 7.71. ESI⁺ MS: m/z 831.6 {M + 2Na}²⁺.

[Eu(LPhBr)₃·2.5H₂O]. The complex precipitated on mixing of reagents: 51 mg (0.037 mmol, 88%) from HLPPhBr (50 mg, 0.127 mmol), NaOH (5.1 mg, 0.127 mmol), and $\text{EuCl}_3 \cdot 6\text{H}_2\text{O}$ (15.5 mg, 0.042 mmol). Anal. Calcd for $\text{C}_{57}\text{H}_{33}\text{Br}_3\text{EuN}_9\text{O}_6 \cdot 2.5\text{H}_2\text{O}$ (MW 1376.64): C, 49.73; H, 2.78; N, 9.16. Found: C, 49.85; H, 2.74; N, 8.75. ESI⁺ MS: m/z 1354.4 {M + Na}⁺, 688.7 {M + 2Na}²⁺.

[Eu(LPhBu)₃·1.5H₂O]. The complex was precipitated with water (8 mL): 45 mg (0.035 mmol, 79%) from HLPPhBu·0.5H₂O (50 mg, 0.131 mmol), NaOH (5.25 mg, 0.131 mmol), and $\text{EuCl}_3 \cdot 6\text{H}_2\text{O}$ (16.05 mg, 0.044 mmol). Anal. Calcd for $\text{C}_{69}\text{H}_{60}\text{EuN}_9\text{O}_6 \cdot 1.5\text{H}_2\text{O}$ (MW 1290.26): C, 64.23; H, 4.92; N, 9.77. Found: C, 64.18; H, 4.83; N, 9.65. ESI⁺ MS: m/z 1264.8 {M + H}⁺, 632.4 {M + 2H}²⁺.

[Eu(LPhO8)₃·2H₂O]. The complex was precipitated with water (2.5 mL): 41 mg (0.027 mmol, 71%) from HLPPhO8 (50 mg, 0.113 mmol), NaOH (4.51 mg, 0.113 mmol), and $\text{EuCl}_3 \cdot 6\text{H}_2\text{O}$ (13.77 mg, 0.038 mmol). Anal. Calcd for $\text{C}_{81}\text{H}_{84}\text{EuN}_9\text{O}_9 \cdot 2\text{H}_2\text{O}$ (MW 1515.58): C, 64.19; H, 5.85; N, 8.32. Found: C, 64.05; H, 5.96; N, 8.22. ESI⁺ MS: m/z 763.0 {M + 2Na}²⁺.

[Eu(LPhX)₃·1.5H₂O]. The complex was precipitated with water (3 mL): 25 mg (0.017 mmol, 73%) from HLPPhX (30 mg, 0.068 mmol), NaOH (2.71 mg, 0.068 mmol), and $\text{EuCl}_3 \cdot 6\text{H}_2\text{O}$ (8.3 mg, 0.0227 mmol). Anal. Calcd for $\text{C}_{81}\text{H}_{84}\text{EuN}_9\text{O}_9 \cdot 1.5\text{H}_2\text{O}$ (MW 1506.58): C, 64.57; H, 5.82; N, 8.37. Found: C, 64.74; H, 5.92; N, 8.37. ESI⁺ MS: m/z 763.0 {M + 2Na}²⁺.

[Eu(LBiphX)₃]. The complex precipitated on mixing of reagents: 46 mg (0.027 mmol, 84%) from HLBiphX (50 mg, 0.096 mmol), NaOH (3.85 mg, 0.096 mmol), and $\text{EuCl}_3 \cdot 6\text{H}_2\text{O}$ (11.8 mg, 0.032 mmol). Anal. Calcd for $\text{C}_{99}\text{H}_{96}\text{EuN}_9\text{O}_9$ (MW 1707.84): C, 69.62; H, 5.67; N, 7.38. Found: C, 69.49; H, 5.89; N, 7.37. ESI⁺ MS: m/z 877.1 {M + 2Na}²⁺.

[Eu(LNapX)₃·H₂O]. The complex was precipitated with water (1 mL): 46 mg (0.28 mmol, 82%) from HLNapX (50 mg, 0.10 mmol), NaOH (4.05 mg, 0.10 mmol), and $\text{EuCl}_3 \cdot 6\text{H}_2\text{O}$ (12.4 mg, 0.034 mmol). Anal. Calcd for $\text{C}_{93}\text{H}_{90}\text{EuN}_9\text{O}_9 \cdot \text{H}_2\text{O}$ (MW 1647.74): C, 67.79; H, 5.63; N, 7.65. Found: C, 67.85; H, 5.85; N, 7.62. ESI⁺ MS: m/z 1631.1 {M + H}⁺, 816.1 {M + 2H}²⁺.

Acknowledgment. This research is supported by a grant from the Swiss National Science Foundation (No. 200020_119866/1). J.C.B. thanks the WCU (World Class University) program from the National Science Foundation of Korea (Ministry of Education, Science, and Technology) for Grant R31-10035.

Supporting Information Available: Synthesis of the ligand precursors; absorption and luminescence spectra; ¹H and ¹³C NMR spectra; CIF files of the crystal structures, CCDC 762688 and 762689. This material is available free of charge via the Internet at <http://pubs.acs.org>.